

# Evidence for $e^+e^- \rightarrow \gamma\chi_{c1,2}$ at center-of-mass energies from 4.009 to 4.360 GeV

M. Ablikim<sup>1</sup>, M. N. Achasov<sup>8,a</sup>, X. C. Ai<sup>1</sup>, O. Albayrak<sup>4</sup>, M. Albrecht<sup>3</sup>, D. J. Ambrose<sup>43</sup>, A. Amoroso<sup>47A,47C</sup>, F. F. An<sup>1</sup>, Q. An<sup>44</sup>, J. Z. Bai<sup>1</sup>, R. Baldini Ferroli<sup>19A</sup>, Y. Ban<sup>30</sup>, D. W. Bennett<sup>18</sup>, J. V. Bennett<sup>4</sup>, M. Bertani<sup>19A</sup>, D. Bettoni<sup>20A</sup>, J. M. Bian<sup>42</sup>, F. Bianchi<sup>47A,47C</sup>, E. Boger<sup>22,g</sup>, O. Bondarenko<sup>24</sup>, I. Boyko<sup>22</sup>, R. A. Briere<sup>4</sup>, H. Cai<sup>49</sup>, X. Cai<sup>1</sup>, O. Cakir<sup>39A</sup>, A. Calcaterra<sup>19A</sup>, G. F. Cao<sup>1</sup>, S. A. Cetin<sup>39B</sup>, J. F. Chang<sup>1</sup>, G. Chelkov<sup>22,b</sup>, G. Chen<sup>1</sup>, H. S. Chen<sup>1</sup>, H. Y. Chen<sup>2</sup>, J. C. Chen<sup>1</sup>, M. L. Chen<sup>1</sup>, S. J. Chen<sup>28</sup>, X. Chen<sup>1</sup>, X. R. Chen<sup>25</sup>, Y. B. Chen<sup>1</sup>, H. P. Cheng<sup>16</sup>, X. K. Chu<sup>30</sup>, G. Cibinetto<sup>20A</sup>, D. Cronin-Hennessy<sup>42</sup>, H. L. Dai<sup>1</sup>, J. P. Dai<sup>33</sup>, A. Dbeyssi<sup>13</sup>, D. Dedovich<sup>22</sup>, Z. Y. Deng<sup>1</sup>, A. Denig<sup>21</sup>, I. Denysenko<sup>22</sup>, M. Destefanis<sup>47A,47C</sup>, F. De Mori<sup>47A,47C</sup>, Y. Ding<sup>26</sup>, C. Dong<sup>29</sup>, J. Dong<sup>1</sup>, L. Y. Dong<sup>1</sup>, M. Y. Dong<sup>1</sup>, S. X. Du<sup>51</sup>, P. F. Duan<sup>1</sup>, J. Z. Fan<sup>38</sup>, J. Fang<sup>1</sup>, S. S. Fang<sup>1</sup>, X. Fang<sup>44</sup>, Y. Fang<sup>1</sup>, L. Fava<sup>47B,47C</sup>, F. Feldbauer<sup>21</sup>, G. Felici<sup>19A</sup>, C. Q. Feng<sup>44</sup>, E. Fioravanti<sup>20A</sup>, C. D. Fu<sup>1</sup>, Q. Gao<sup>1</sup>, Y. Gao<sup>38</sup>, I. Garzia<sup>20A</sup>, K. Goetzen<sup>9</sup>, W. X. Gong<sup>1</sup>, W. Gradl<sup>21</sup>, M. Greco<sup>47A,47C</sup>, M. H. Gu<sup>1</sup>, Y. T. Gu<sup>11</sup>, Y. H. Guan<sup>1</sup>, A. Q. Guo<sup>1</sup>, L. B. Guo<sup>27</sup>, T. Guo<sup>27</sup>, Y. Guo<sup>1</sup>, Y. P. Guo<sup>21</sup>, Z. Haddadi<sup>24</sup>, A. Hafner<sup>21</sup>, S. Han<sup>49</sup>, Y. L. Han<sup>1</sup>, F. A. Harris<sup>41</sup>, K. L. He<sup>1</sup>, Z. Y. He<sup>29</sup>, T. Held<sup>3</sup>, Y. K. Heng<sup>1</sup>, Z. L. Hou<sup>1</sup>, C. Hu<sup>27</sup>, H. M. Hu<sup>1</sup>, J. F. Hu<sup>47A</sup>, T. Hu<sup>1</sup>, Y. Hu<sup>1</sup>, G. M. Huang<sup>5</sup>, G. S. Huang<sup>44</sup>, H. P. Huang<sup>49</sup>, J. S. Huang<sup>14</sup>, X. T. Huang<sup>32</sup>, Y. Huang<sup>28</sup>, T. Hussain<sup>46</sup>, Q. Ji<sup>1</sup>, Q. P. Ji<sup>29</sup>, X. B. Ji<sup>1</sup>, X. L. Ji<sup>1</sup>, L. L. Jiang<sup>1</sup>, L. W. Jiang<sup>49</sup>, X. S. Jiang<sup>1</sup>, J. B. Jiao<sup>32</sup>, Z. Jiao<sup>16</sup>, D. P. Jin<sup>1</sup>, S. Jin<sup>1</sup>, T. Johansson<sup>48</sup>, A. Julin<sup>42</sup>, N. Kalantar-Nayestanaki<sup>24</sup>, X. L. Kang<sup>1</sup>, X. S. Kang<sup>29</sup>, M. Kavatsyuk<sup>24</sup>, B. C. Ke<sup>4</sup>, R. Kliemt<sup>13</sup>, B. Kloss<sup>21</sup>, O. B. Kolcu<sup>39B,c</sup>, B. Kopf<sup>3</sup>, M. Kornicer<sup>41</sup>, W. Kuehn<sup>23</sup>, A. Kupsc<sup>48</sup>, W. Lai<sup>1</sup>, J. S. Lange<sup>23</sup>, M. Lara<sup>18</sup>, P. Larin<sup>13</sup>, C. H. Li<sup>1</sup>, Cheng Li<sup>44</sup>, D. M. Li<sup>51</sup>, F. Li<sup>1</sup>, G. Li<sup>1</sup>, H. B. Li<sup>1</sup>, J. C. Li<sup>1</sup>, Jin Li<sup>31</sup>, K. Li<sup>12</sup>, K. Li<sup>32</sup>, P. R. Li<sup>40</sup>, T. Li<sup>32</sup>, W. D. Li<sup>1</sup>, W. G. Li<sup>1</sup>, X. L. Li<sup>32</sup>, X. M. Li<sup>11</sup>, X. N. Li<sup>1</sup>, X. Q. Li<sup>29</sup>, Z. B. Li<sup>37</sup>, H. Liang<sup>44</sup>, Y. F. Liang<sup>35</sup>, Y. T. Liang<sup>23</sup>, G. R. Liao<sup>10</sup>, D. X. Lin<sup>13</sup>, B. J. Liu<sup>1</sup>, C. L. Liu<sup>4</sup>, C. X. Liu<sup>1</sup>, F. H. Liu<sup>34</sup>, Fang Liu<sup>1</sup>, Feng Liu<sup>5</sup>, H. B. Liu<sup>11</sup>, H. H. Liu<sup>15</sup>, H. H. Liu<sup>1</sup>, H. M. Liu<sup>1</sup>, J. Liu<sup>1</sup>, J. P. Liu<sup>49</sup>, J. Y. Liu<sup>1</sup>, K. Liu<sup>38</sup>, K. Y. Liu<sup>26</sup>, L. D. Liu<sup>30</sup>, P. L. Liu<sup>1</sup>, Q. Liu<sup>40</sup>, S. B. Liu<sup>44</sup>, X. Liu<sup>25</sup>, X. X. Liu<sup>40</sup>, Y. B. Liu<sup>29</sup>, Z. A. Liu<sup>1</sup>, Zhiqiang Liu<sup>1</sup>, Zhiqing Liu<sup>21</sup>, H. Loehner<sup>24</sup>, X. C. Lou<sup>1,d</sup>, H. J. Lu<sup>16</sup>, J. G. Lu<sup>1</sup>, R. Q. Lu<sup>17</sup>, Y. Lu<sup>1</sup>, Y. P. Lu<sup>1</sup>, C. L. Luo<sup>27</sup>, M. X. Luo<sup>50</sup>, T. Luo<sup>41</sup>, X. L. Luo<sup>1</sup>, M. Lv<sup>1</sup>, X. R. Lyu<sup>40</sup>, F. C. Ma<sup>26</sup>, H. L. Ma<sup>1</sup>, L. L. Ma<sup>32</sup>, Q. M. Ma<sup>1</sup>, S. Ma<sup>1</sup>, T. Ma<sup>1</sup>, X. N. Ma<sup>29</sup>, X. Y. Ma<sup>1</sup>, F. E. Maas<sup>13</sup>, M. Maggiora<sup>47A,47C</sup>, Q. A. Malik<sup>46</sup>, Y. J. Mao<sup>30</sup>, Z. P. Mao<sup>1</sup>, S. Marcello<sup>47A,47C</sup>, J. G. Messchendorp<sup>24</sup>, J. Min<sup>1</sup>, T. J. Min<sup>1</sup>, R. E. Mitchell<sup>18</sup>, X. H. Mo<sup>1</sup>, Y. J. Mo<sup>5</sup>, C. Morales Morales<sup>13</sup>, K. Moriya<sup>8,a</sup>, N. Yu. Muchnoi<sup>8,a</sup>, H. Muramatsu<sup>42</sup>, Y. Nefedov<sup>22</sup>, F. Nerling<sup>13</sup>, I. B. Nikolaev<sup>8,a</sup>, Z. Ning<sup>1</sup>, S. Nisar<sup>7</sup>, S. L. Niu<sup>1</sup>, X. Y. Niu<sup>1</sup>, S. L. Olsen<sup>31</sup>, Q. Ouyang<sup>1</sup>, S. Pacetti<sup>19B</sup>, P. Patteri<sup>19A</sup>, M. Pelizaeus<sup>3</sup>, H. P. Peng<sup>44</sup>, K. Peters<sup>9</sup>, J. L. Ping<sup>27</sup>, R. G. Ping<sup>1</sup>, R. Poling<sup>42</sup>, Y. N. Pu<sup>17</sup>, M. Qi<sup>28</sup>, S. Qian<sup>1</sup>, C. F. Qiao<sup>40</sup>, L. Q. Qin<sup>32</sup>, N. Qin<sup>49</sup>, X. S. Qin<sup>1</sup>, Y. Qin<sup>30</sup>, Z. H. Qin<sup>1</sup>, J. F. Qiu<sup>1</sup>, K. H. Rashid<sup>46</sup>, C. F. Redmer<sup>21</sup>, H. L. Ren<sup>17</sup>, M. Ripka<sup>21</sup>, G. Rong<sup>1</sup>, X. D. Ruan<sup>11</sup>, V. Santoro<sup>20A</sup>, A. Sarantsev<sup>22,e</sup>, M. Savrié<sup>20B</sup>, K. Schoenning<sup>48</sup>, S. Schumann<sup>21</sup>, W. Shan<sup>30</sup>, M. Shao<sup>44</sup>, C. P. Shen<sup>2</sup>, P. X. Shen<sup>29</sup>, X. Y. Shen<sup>1</sup>, H. Y. Sheng<sup>1</sup>, M. R. Shepherd<sup>18</sup>, W. M. Song<sup>1</sup>, X. Y. Song<sup>1</sup>, S. Sosio<sup>47A,47C</sup>, S. Spataro<sup>47A,47C</sup>, B. Spruck<sup>23</sup>, G. X. Sun<sup>1</sup>, J. F. Sun<sup>14</sup>, S. S. Sun<sup>1</sup>, Y. J. Sun<sup>44</sup>, Y. Z. Sun<sup>1</sup>, Z. J. Sun<sup>1</sup>, Z. T. Sun<sup>18</sup>, C. J. Tang<sup>35</sup>, X. Tang<sup>1</sup>, I. Tapan<sup>39C</sup>, E. H. Thorndike<sup>43</sup>, M. Tiemens<sup>24</sup>, D. Toth<sup>42</sup>, M. Ullrich<sup>23</sup>, I. Uman<sup>39B</sup>, G. S. Varner<sup>41</sup>, B. Wang<sup>29</sup>, B. L. Wang<sup>40</sup>, D. Wang<sup>30</sup>, D. Y. Wang<sup>30</sup>, K. Wang<sup>1</sup>, L. L. Wang<sup>1</sup>, L. S. Wang<sup>1</sup>, M. Wang<sup>32</sup>, P. Wang<sup>1</sup>, P. L. Wang<sup>1</sup>, Q. J. Wang<sup>1</sup>, S. G. Wang<sup>30</sup>, W. Wang<sup>1</sup>, X. F. Wang<sup>38</sup>, Y. D. Wang<sup>19A</sup>, Y. F. Wang<sup>1</sup>, Y. Q. Wang<sup>21</sup>, Z. Wang<sup>1</sup>, Z. G. Wang<sup>1</sup>, Z. H. Wang<sup>44</sup>, Z. Y. Wang<sup>1</sup>, D. H. Wei<sup>10</sup>, J. B. Wei<sup>30</sup>, P. Weidenkaff<sup>21</sup>, S. P. Wen<sup>1</sup>, U. Wiedner<sup>3</sup>, M. Wolke<sup>48</sup>, L. H. Wu<sup>1</sup>, Z. Wu<sup>1</sup>, L. G. Xia<sup>38</sup>, Y. Xia<sup>17</sup>, D. Xiao<sup>1</sup>, Z. J. Xiao<sup>27</sup>, Y. G. Xie<sup>1</sup>, G. F. Xu<sup>1</sup>, L. Xu<sup>1</sup>, Q. J. Xu<sup>12</sup>, Q. N. Xu<sup>40</sup>, X. P. Xu<sup>36</sup>, L. Yan<sup>44</sup>, W. B. Yan<sup>44</sup>, W. C. Yan<sup>44</sup>, Y. H. Yan<sup>17</sup>, H. X. Yang<sup>1</sup>, L. Yang<sup>49</sup>, Y. Yang<sup>5</sup>, Y. X. Yang<sup>10</sup>, H. Ye<sup>1</sup>, M. Ye<sup>1</sup>, M. H. Ye<sup>6</sup>, J. H. Yin<sup>1</sup>, B. X. Yu<sup>1</sup>, C. X. Yu<sup>29</sup>, H. W. Yu<sup>30</sup>, J. S. Yu<sup>25</sup>, C. Z. Yuan<sup>1</sup>, W. L. Yuan<sup>28</sup>, Y. Yuan<sup>1</sup>, A. Yuncu<sup>39B,f</sup>, A. A. Zafar<sup>46</sup>, A. Zallo<sup>19A</sup>, Y. Zeng<sup>17</sup>, B. X. Zhang<sup>1</sup>, B. Y. Zhang<sup>1</sup>, C. Zhang<sup>28</sup>, C. C. Zhang<sup>1</sup>, D. H. Zhang<sup>1</sup>, H. H. Zhang<sup>37</sup>, H. Y. Zhang<sup>1</sup>, J. J. Zhang<sup>1</sup>, J. L. Zhang<sup>1</sup>, J. Q. Zhang<sup>1</sup>, J. W. Zhang<sup>1</sup>, J. Y. Zhang<sup>1</sup>, J. Z. Zhang<sup>1</sup>, K. Zhang<sup>1</sup>, L. Zhang<sup>1</sup>, S. H. Zhang<sup>1</sup>, X. J. Zhang<sup>1</sup>, X. Y. Zhang<sup>32</sup>, Y. Zhang<sup>1</sup>, Y. H. Zhang<sup>1</sup>, Z. H. Zhang<sup>5</sup>, Z. P. Zhang<sup>44</sup>, Z. Y. Zhang<sup>49</sup>, G. Zhao<sup>1</sup>, J. W. Zhao<sup>1</sup>, J. Y. Zhao<sup>1</sup>, J. Z. Zhao<sup>1</sup>, Lei Zhao<sup>44</sup>, Ling Zhao<sup>1</sup>, M. G. Zhao<sup>29</sup>, Q. Zhao<sup>1</sup>, S. J. Zhao<sup>51</sup>, T. C. Zhao<sup>1</sup>, Y. B. Zhao<sup>1</sup>, Z. G. Zhao<sup>44</sup>, A. Zhemchugov<sup>22,g</sup>, B. Zheng<sup>45</sup>, J. P. Zheng<sup>1</sup>, W. J. Zheng<sup>32</sup>, Y. H. Zheng<sup>40</sup>, B. Zhong<sup>27</sup>, L. Zhou<sup>1</sup>, Li Zhou<sup>29</sup>, X. Zhou<sup>49</sup>, X. K. Zhou<sup>44</sup>, X. R. Zhou<sup>44</sup>, X. Y. Zhou<sup>1</sup>, K. Zhu<sup>1</sup>, K. J. Zhu<sup>1</sup>, S. Zhu<sup>1</sup>, X. L. Zhu<sup>38</sup>, Y. C. Zhu<sup>44</sup>, Y. S. Zhu<sup>1</sup>, Z. A. Zhu<sup>1</sup>, J. Zhuang<sup>1</sup>, B. S. Zou<sup>1</sup>, J. H. Zou<sup>1</sup>

(BESIII Collaboration)

<sup>1</sup> Institute of High Energy Physics, Beijing 100049, People's Republic of China

<sup>2</sup> Beihang University, Beijing 100191, People's Republic of China

<sup>3</sup> Bochum Ruhr-University, D-44780 Bochum, Germany

<sup>4</sup> Carnegie Mellon University, Pittsburgh, Pennsylvania 15213, USA

<sup>5</sup> Central China Normal University, Wuhan 430079, People's Republic of China

<sup>6</sup> China Center of Advanced Science and Technology, Beijing 100190, People's Republic of China

<sup>7</sup> COMSATS Institute of Information Technology, Lahore, Defence Road, Off Raiwind Road, 54000 Lahore, Pakistan

<sup>8</sup> G.I. Budker Institute of Nuclear Physics SB RAS (BINP), Novosibirsk 630090, Russia

<sup>9</sup> GSI Helmholtzcentre for Heavy Ion Research GmbH, D-64291 Darmstadt, Germany

<sup>10</sup> Guangxi Normal University, Guilin 541004, People's Republic of China

<sup>11</sup> GuangXi University, Nanning 530004, People's Republic of China

<sup>12</sup> Hangzhou Normal University, Hangzhou 310036, People's Republic of China

<sup>13</sup> Helmholtz Institute Mainz, Johann-Joachim-Becher-Weg 45, D-55099 Mainz, Germany

<sup>14</sup> Henan Normal University, Xinxiang 453007, People's Republic of China

<sup>15</sup> Henan University of Science and Technology, Luoyang 471003, People's Republic of China

<sup>16</sup> Huangshan College, Huangshan 245000, People's Republic of China

<sup>17</sup> Hunan University, Changsha 410082, People's Republic of China

<sup>18</sup> Indiana University, Bloomington, Indiana 47405, USA

<sup>19</sup> (A)INFN Laboratori Nazionali di Frascati, I-00044, Frascati, Italy; (B)INFN and University of Perugia, I-06100, Perugia, Italy

<sup>20</sup> (A)INFN Sezione di Ferrara, I-44122, Ferrara, Italy; (B)University of Ferrara, I-44122, Ferrara, Italy

- <sup>21</sup> Johannes Gutenberg University of Mainz, Johann-Joachim-Becher-Weg 45, D-55099 Mainz, Germany
- <sup>22</sup> Joint Institute for Nuclear Research, 141980 Dubna, Moscow region, Russia
- <sup>23</sup> Justus Liebig University Giessen, II. Physikalisches Institut, Heinrich-Buff-Ring 16, D-35392 Giessen, Germany
- <sup>24</sup> KVI-CART, University of Groningen, NL-9747 AA Groningen, The Netherlands
- <sup>25</sup> Lanzhou University, Lanzhou 730000, People's Republic of China
- <sup>26</sup> Liaoning University, Shenyang 110036, People's Republic of China
- <sup>27</sup> Nanjing Normal University, Nanjing 210023, People's Republic of China
- <sup>28</sup> Nanjing University, Nanjing 210093, People's Republic of China
- <sup>29</sup> Nankai University, Tianjin 300071, People's Republic of China
- <sup>30</sup> Peking University, Beijing 100871, People's Republic of China
- <sup>31</sup> Seoul National University, Seoul, 151-747 Korea
- <sup>32</sup> Shandong University, Jinan 250100, People's Republic of China
- <sup>33</sup> Shanghai Jiao Tong University, Shanghai 200240, People's Republic of China
- <sup>34</sup> Shanxi University, Taiyuan 030006, People's Republic of China
- <sup>35</sup> Sichuan University, Chengdu 610064, People's Republic of China
- <sup>36</sup> Soochow University, Suzhou 215006, People's Republic of China
- <sup>37</sup> Sun Yat-Sen University, Guangzhou 510275, People's Republic of China
- <sup>38</sup> Tsinghua University, Beijing 100084, People's Republic of China
- <sup>39</sup> (A)Ankara University, Dogol Caddesi, 06100 Tandogan, Ankara, Turkey; (B)Dogus University, 34722 Istanbul, Turkey; (C)Uludag University, 16059 Bursa, Turkey
- <sup>40</sup> University of Chinese Academy of Sciences, Beijing 100049, People's Republic of China
- <sup>41</sup> University of Hawaii, Honolulu, Hawaii 96822, USA
- <sup>42</sup> University of Minnesota, Minneapolis, Minnesota 55455, USA
- <sup>43</sup> University of Rochester, Rochester, New York 14627, USA
- <sup>44</sup> University of Science and Technology of China, Hefei 230026, People's Republic of China
- <sup>45</sup> University of South China, Hengyang 421001, People's Republic of China
- <sup>46</sup> University of the Punjab, Lahore-54590, Pakistan
- <sup>47</sup> (A)University of Turin, I-10125, Turin, Italy; (B)University of Eastern Piedmont, I-15121, Alessandria, Italy; (C)INFN, I-10125, Turin, Italy
- <sup>48</sup> Uppsala University, Box 516, SE-75120 Uppsala, Sweden
- <sup>49</sup> Wuhan University, Wuhan 430072, People's Republic of China
- <sup>50</sup> Zhejiang University, Hangzhou 310027, People's Republic of China
- <sup>51</sup> Zhengzhou University, Zhengzhou 450001, People's Republic of China
- <sup>a</sup> Also at the Novosibirsk State University, Novosibirsk, 630090, Russia
- <sup>b</sup> Also at the Moscow Institute of Physics and Technology, Moscow 141700, Russia and at the Functional Electronics Laboratory, Tomsk State University, Tomsk, 634050, Russia
- <sup>c</sup> Currently at Istanbul Arel University, Kucukcekmece, Istanbul, Turkey
- <sup>d</sup> Also at University of Texas at Dallas, Richardson, Texas 75083, USA
- <sup>e</sup> Also at the PNPI, Gatchina 188300, Russia
- <sup>f</sup> Also at Bogazici University, 34342 Istanbul, Turkey
- <sup>g</sup> Also at the Moscow Institute of Physics and Technology, Moscow 141700, Russia

Using data samples collected at center-of-mass energies of  $\sqrt{s} = 4.009, 4.230, 4.260$ , and  $4.360$  GeV with the BESIII detector operating at the BEPCII collider, we perform a search for the process  $e^+e^- \rightarrow \gamma\chi_{cJ}$  ( $J = 0, 1, 2$ ) and find evidence for  $e^+e^- \rightarrow \gamma\chi_{c1}$  and  $e^+e^- \rightarrow \gamma\chi_{c2}$  with statistical significances of  $3.0\sigma$  and  $3.4\sigma$ , respectively. The Born cross sections  $\sigma^B(e^+e^- \rightarrow \gamma\chi_{cJ})$ , as well as their upper limits at the 90% confidence level are determined at each center-of-mass energy.

PACS numbers: 14.40.Pq, 13.25.Gv, 13.66.Bc

## I. INTRODUCTION

The charmonium-like state  $Y(4260)$  was first observed in the initial state radiation (ISR) process  $e^+e^- \rightarrow \gamma_{ISR}\pi^+\pi^-J/\psi$  by BaBar [1], and later confirmed by the CLEO [2] and Belle [3] experiments. Recently, both BaBar and Belle updated their results with full data sets, respectively, and further confirmed the existence of the  $Y(4260)$  [4, 5].

Since it is produced through ISR in  $e^+e^-$  annihilation, the  $Y(4260)$  has the quantum numbers  $J^{PC} = 1^{--}$ . However, there seems to be no  $c\bar{c}$  slot available for the  $Y(4260)$  in the conventional charmonium family [6]. In addition, a number of unusual features, such as a strong coupling to hidden-charm final states, suggest that the  $Y(4260)$  is a non-conventional  $c\bar{c}$  meson. Possible interpretations of this state can be found in Refs. [7–11], but all need further experimental input.

Most previous studies of the  $Y(4260)$  have utilized hadronic transitions. Besides the clear signal observed in the  $\pi^+\pi^-J/\psi$  decay mode, the Belle experiment failed to find evidence of the  $Y(4260)$  via the  $e^+e^- \rightarrow \gamma_{ISR}\eta J/\psi$  process [12]. Based on  $13.2 \text{ pb}^{-1}$  of  $e^+e^-$  data collected at  $\sqrt{s} = 4.260 \text{ GeV}$ , the CLEO experiment investigated fourteen hadronic decay channels, but only few decay modes had a significance more than  $3\sigma$  [13]. The BESIII Collaboration first observed the process  $e^+e^- \rightarrow \gamma X(3872)$  using data samples taken between  $\sqrt{s} = 4.009$  and  $4.420 \text{ GeV}$  [14], which strongly supports the existence of the radiative transition decays of the  $Y(4260)$ . To further understand the nature of the  $Y(4260)$  state, an investigation into the radiative transitions between the  $Y(4260)$  and other lower mass charmonium states, like the  $\chi_{cJ}$  ( $J = 0, 1, 2$ ), is important [15, 16]. The cross sections of  $e^+e^- \rightarrow \gamma\chi_{cJ}$  have been evaluated theoretically within the framework of NRQCD [16]. Experimentally, the only existing investigation comes from the CLEO experiment [13], which did not observe a signal. The large data sample collected with the BESIII detector provides a good opportunity to deeply investigate these decay modes, which may shed more light on the properties of the  $Y(4260)$ .

In this paper, we report on a search for  $e^+e^- \rightarrow \gamma\chi_{cJ}$  ( $J = 0, 1, 2$ ) based on the large  $e^+e^-$  annihilation data samples collected with the BESIII detector at center-of-mass energies (CME)  $\sqrt{s} = 4.009, 4.230, 4.260$ , and  $4.360 \text{ GeV}$ , where the  $\chi_{cJ}$  is reconstructed by its  $\gamma J/\psi$  decay mode, and the  $J/\psi$  is by its decay to  $\mu^+\mu^-$ . The decay  $J/\psi \rightarrow e^+e^-$  is not considered in this analysis due to the high background of Bhabha events. The corresponding luminosities of the data samples at different CME used in this analysis are listed in Table I.

TABLE I. The center-of-mass energy and Luminosity of each data sample.

$\sqrt{s} \text{ (GeV)}$	luminosity ( $\text{pb}^{-1}$ )
4.009	482
4.230	1047
4.260	826
4.360	540

## II. BESIII DETECTOR AND MONTE CARLO

The BESIII detector at the BEPCII collider [17] is a large solid-angle magnetic spectrometer with a geometrical acceptance of 93% of  $4\pi$  solid angle consisting of four main components. The innermost is a small-cell, helium-based (40% He, 60%  $\text{C}_3\text{H}_8$ ) main drift chamber (MDC) with 43 layers providing an average single-hit resolution of  $135 \mu\text{m}$ . The resulting charged-particle momentum resolution for a 1 T magnetic field setting is 0.5% at  $1.0 \text{ GeV}/c$ , and the resolution on the ionization energy loss information ( $dE/dx$ ) is better than 6%. The next detector, moving radially outwards, is a time-of-flight (TOF) system constructed of 5 cm thick plastic

scintillators, with 176 detectors of 2.4 m length in two layers in the barrel and 96 fan-shaped detectors in the end-caps. The barrel (end-cap) time resolution of 80 ps (110 ps) provides a  $2\sigma$   $K/\pi$  separation for momenta up to  $1.0 \text{ GeV}$ . Continuing outward, we have an electromagnetic calorimeter (EMC) consisting of 6240 CsI(Tl) crystals in a cylindrical barrel structure and two end-caps. The energy resolution at  $1.0 \text{ GeV}$  is 2.5% (5%) and the position resolution is 6 mm (9 mm) in the barrel (end-caps). Finally, the muon counter (MUC) consists of  $1000 \text{ m}^2$  of Resistive Plate Chambers (RPCs) in nine barrel and eight end-cap layers, which provides a 2 cm position resolution.

A GEANT4 [18] based Monte Carlo (MC) simulation software, which includes the geometric description of the detector and the detector response, is used to optimize the event selection criteria, determine the detection efficiency, and estimate the potential backgrounds. Signal MC samples of  $e^+e^- \rightarrow \gamma\chi_{cJ}$  are generated for each CME according to the electric-dipole (E1) transition assumption [19]. Effects of ISR are simulated with KKMC [20] by assuming that  $\gamma\chi_{cJ}$  is produced via  $Y(4260)$  decays, where the  $Y(4260)$  is described by a Breit-Wigner function with resonance parameters from the Particle Data Group (PDG) [21]. For the background studies, an ‘inclusive’  $Y(4260)$  MC sample equivalent to  $500 \text{ pb}^{-1}$  integrated luminosity is generated which includes the  $Y(4260)$  resonance, ISR production of the known vector charmonium states, and events driven by QED processes. The known decay modes are generated with EvtGen [19] with branching fractions set to their world average values in the PDG [21], and the remaining events are generated with Lundcharm [22] or PYTHIA [23].

## III. EVENT SELECTION

Charged tracks are reconstructed in the MDC. For each good charged track, the polar angle must satisfy  $|\cos\theta| < 0.93$ , and the point of closest approach to the interaction point must be within  $\pm 10 \text{ cm}$  in the beam direction and within  $\pm 1 \text{ cm}$  in the plane perpendicular to the beam direction. The number of good charged tracks is required to be two with a zero net charge. Charged tracks are identified as muons if they have  $E/p < 0.35$  and  $p > 1.0 \text{ GeV}/c$ , where  $E$  is the energy deposited in the EMC and  $p$  is the momentum measured by the MDC.

Photons are reconstructed from isolated showers in the EMC that are at least 20 degrees away from any of the charged tracks. To improve the reconstruction efficiency and the energy resolution, the energy deposited in the nearby TOF counters is included. Photon candidates are required to have energy greater than 25 MeV in the EMC barrel region ( $|\cos\theta| < 0.8$ ), and 50 MeV in the end-cap region ( $0.86 < |\cos\theta| < 0.92$ ). In order to suppress electronic noise and energy deposits that are unrelated to the event, the EMC time  $t$  of the photon candidates must be in coincidence with collision events within the range  $0 \leq t \leq 700 \text{ ns}$ . At least two photon candidates in the final state are required.

To improve the momentum resolution and to reduce backgrounds, a kinematic fit with five constraints (5C-fit) is performed under the  $e^+e^- \rightarrow \gamma\gamma\mu^+\mu^-$  hypothesis, imposing overall energy and momentum conservation and constraining the invariant mass of  $\mu^+\mu^-$  to the nominal  $J/\psi$  mass. Candidates with a  $\chi_{5C}^2 < 40$  are selected for further analysis. If more than one candidate occurs in an event, the one with the smallest  $\chi_{5C}^2$  is selected. Due to the kinematics of the reaction, the first radiative photon from  $e^+e^- \rightarrow \gamma\chi_{cJ}$  has a high energy while the second radiative photon from  $\chi_{cJ} \rightarrow \gamma J/\psi$  has a lower energy at  $\sqrt{s} = 4.230, 4.260$ , and  $4.360$  GeV. The invariant mass of the low energy photon and  $J/\psi$ ,  $M_{\gamma J/\psi}$ , is used to search for  $\chi_{cJ}$  signals. However, for the data sample taken at  $\sqrt{s} = 4.009$  GeV, there is an overlap of the energy distributions of the photons from  $e^+e^- \rightarrow \gamma\chi_{c1,2}$  and from  $\chi_{c1,2}$  decays, as shown in Fig. 1. To separate the overlapping photon spectra, the energy of photons from  $\chi_{c1,2}$  decays is further required to be less than  $0.403$  GeV at  $\sqrt{s} = 4.009$  GeV.

#### IV. BACKGROUND STUDY

The potential backgrounds from  $e^+e^- \rightarrow P + J/\psi$ ,  $P \rightarrow \gamma\gamma$  ( $P = \pi^0, \eta$ , or  $\eta'$ ) can be rejected by requiring  $|M_{\gamma\gamma} - M_{\pi^0}| > 0.025$  GeV/ $c^2$ ,  $|M_{\gamma\gamma} - M_{\eta}| > 0.03$  GeV/ $c^2$  and  $|M_{\gamma\gamma} - M_{\eta'}| > 0.02$  GeV/ $c^2$ , where  $M_{\gamma\gamma}$  is the invariant mass of two selected photons. The background from  $e^+e^- \rightarrow \gamma_{ISR}\psi(3686), \psi(3686) \rightarrow \gamma\chi_{cJ}$  is rejected by applying the 5C kinematic fit. After imposing all the selection criteria above, the remaining dominant background is from radiative dimuon events, which is not expected to peak in the  $M_{\gamma J/\psi}$  distribution. This has been validated by a dedicated simulation study. For other remaining backgrounds, such as  $e^+e^- \rightarrow \pi^0\pi^0 J/\psi$ , only few events (normalized to data luminosity) survive and can be neglected.

#### V. FIT TO THE MASS SPECTRUM

The resulting  $M_{\gamma J/\psi}$  distributions, after applying the above selection criteria, at  $\sqrt{s} = 4.009, 4.230, 4.260$  and  $4.360$  GeV are shown in Figure 2. An unbinned maximum likelihood fit of the  $M_{\gamma J/\psi}$  distribution is performed to extract the numbers of  $\chi_{cJ}$  signal events. In the fit, the shapes of the  $\chi_{cJ}$  signals are described by double Gaussian functions, where the means and the standard deviations of the double Gaussian functions are determined from a fit to the corresponding signal MC samples at  $\sqrt{s} = 4.260$  GeV. These shapes are also used for the other three CME points, as the resolution varies only mildly between  $\sqrt{s} = 4.009 - 4.360$  GeV. This has been validated by MC simulation. Since the dominant background comes from radiative dimuon events, the corresponding MC simulation is used to represent the background shape. To reduce the effect of statistical fluctuations, the dimuon MC shape is smoothed before it is taken as the background function. Figure 2 also shows the fitted results for the  $M_{\gamma J/\psi}$  distribution

at different CME. The number of fitted  $\chi_{cJ}$  signal events, as well as the corresponding statistical significances (calculated by comparing the fit log likelihood values with and without the  $\chi_{cJ}$  signal) at the four CME points are listed in Table II. The same fit is applied to the sum of  $M_{\gamma J/\psi}$  distributions of the four CME points. The statistical significances for  $\chi_{c0}, \chi_{c1}$  and  $\chi_{c2}$  are found to be  $1.2\sigma, 3.0\sigma$  and  $3.4\sigma$ , respectively. As a test, we perform similar analyses to control samples from the  $J/\psi$  sideband regions,  $2.917 < M_{\mu^+\mu^-} < 3.057$  GeV/ $c^2$  and  $3.137 < M_{\mu^+\mu^-} < 3.277$  GeV/ $c^2$ , by constraining the invariant mass of  $\mu^+\mu^-$  to  $3.047$  or  $3.147$  GeV/ $c^2$  in 5C-fit, and find no obvious  $\chi_{cJ}$  signals.

#### VI. RESULTS

The Born cross section at different CME is calculated with

$$\sigma^B(e^+e^- \rightarrow \gamma\chi_{cJ}) = \frac{N^{\text{obs}}}{\mathcal{L} \cdot (1 + \delta^r) \cdot (1 + \delta^v) \cdot \mathcal{B} \cdot \epsilon} \quad (1)$$

where  $N^{\text{obs}}$  is the number of observed events obtained from the fit,  $\mathcal{L}$  is the integrated luminosity,  $1 + \delta^r$  is the radiative correction factor for  $\chi_{cJ}$  with the assumption that the  $e^+e^- \rightarrow \gamma\chi_{cJ}$  cross section follows the  $Y(4260)$  Breit-Wigner line shape [24],  $1 + \delta^v$  is the vacuum polarization factor [25],  $\mathcal{B}$  is the combined branching ratio of  $\chi_{cJ} \rightarrow \gamma J/\psi$  and  $J/\psi \rightarrow \mu^+\mu^-$ , and  $\epsilon$  is the detection efficiency. The detection efficiencies, radiative correction factors as well as the calculated Born cross sections at different CME are shown in Table II. The much lower efficiencies for  $\chi_{c1,2}$  at  $\sqrt{s} = 4.009$  GeV are due to the requirement on the photon energy used to separate the overlapping photon spectra as described in Section III.

Since the  $\chi_{cJ}$  signals are not statistically significant at the individual CME points, we also give in Table II the by assuming the non-existence of signals, the upper limits on the Born cross sections at the 90% confidence level (C. L.) under the assumption that no signals are present. The upper limits are derived using a Bayesian method [21], where the efficiencies are lowered by a factor of  $(1 - \sigma_{\text{sys}})$  to take systematic uncertainties into account.

We also perform a simultaneous fit to the  $M_{\gamma J/\psi}$  distribution at  $\sqrt{s} = 4.009, 4.230, 4.260$ , and  $4.360$  GeV, assuming the production cross section of  $e^+e^- \rightarrow \gamma\chi_{cJ}$  at different CME point follows the line shape of the  $Y(4260)$  state. In the fit, the line shapes of the  $\chi_{cJ}$  signals and the background are as same as those in previous fits, and the number of  $\chi_{cJ}$  events at each CME point is expressed as a function of  $\epsilon_{\text{c.m.}} \mathcal{L}_{\text{c.m.}} R_{\text{c.m.}} (1 + \delta^r)$ , where  $\epsilon_{\text{c.m.}}$  and  $\mathcal{L}_{\text{c.m.}}$  are the detection efficiency and luminosity, respectively, and  $R_{\text{c.m.}}$  is the ratio of the cross section calculated with the  $Y(4260)$  line shape (a Breit-Wigner function with parameters fixed to the PDG values) at different CME points to that at  $\sqrt{s} = 4.260$  GeV. The corresponding fit result is shown in Fig. 3, and the statistical significances for  $\chi_{c0}, \chi_{c1}$  and  $\chi_{c2}$  signals are  $0.0\sigma, 2.4\sigma$  and  $4.0\sigma$ , respectively.



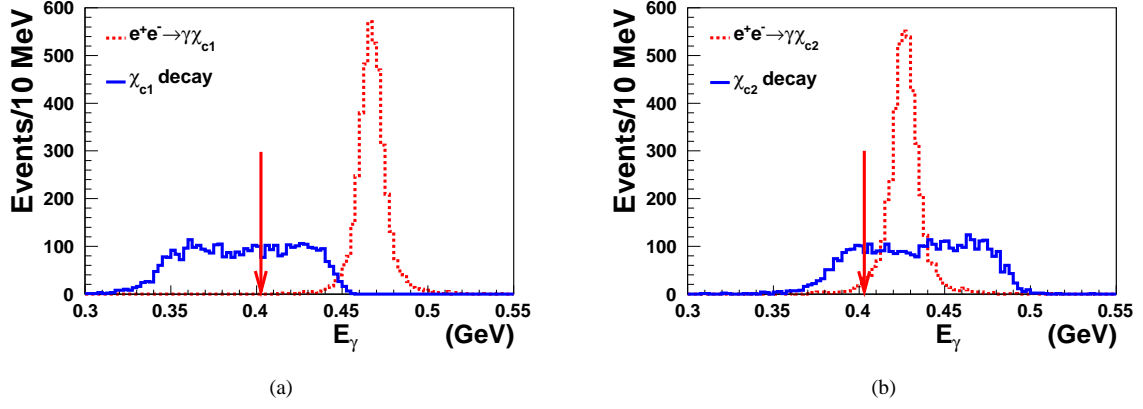


FIG. 1. The distributions of photon energies in the laboratory frame from  $e^+e^- \rightarrow \gamma\chi_{c1,2}$  and from  $\chi_{c1,2}$  decays in the exclusive MC samples of  $e^+e^- \rightarrow \gamma\chi_{c1}, \chi_{c1} \rightarrow \gamma J/\psi$  (a) and  $\chi_{c2}$  (b) at  $\sqrt{s} = 4.009$  GeV. Dashed lines stand for the first radiative photons from  $e^+e^- \rightarrow \gamma\chi_{c1,2}$  and solid lines for the second radiative photons from  $\chi_{c1,2}$  decays.

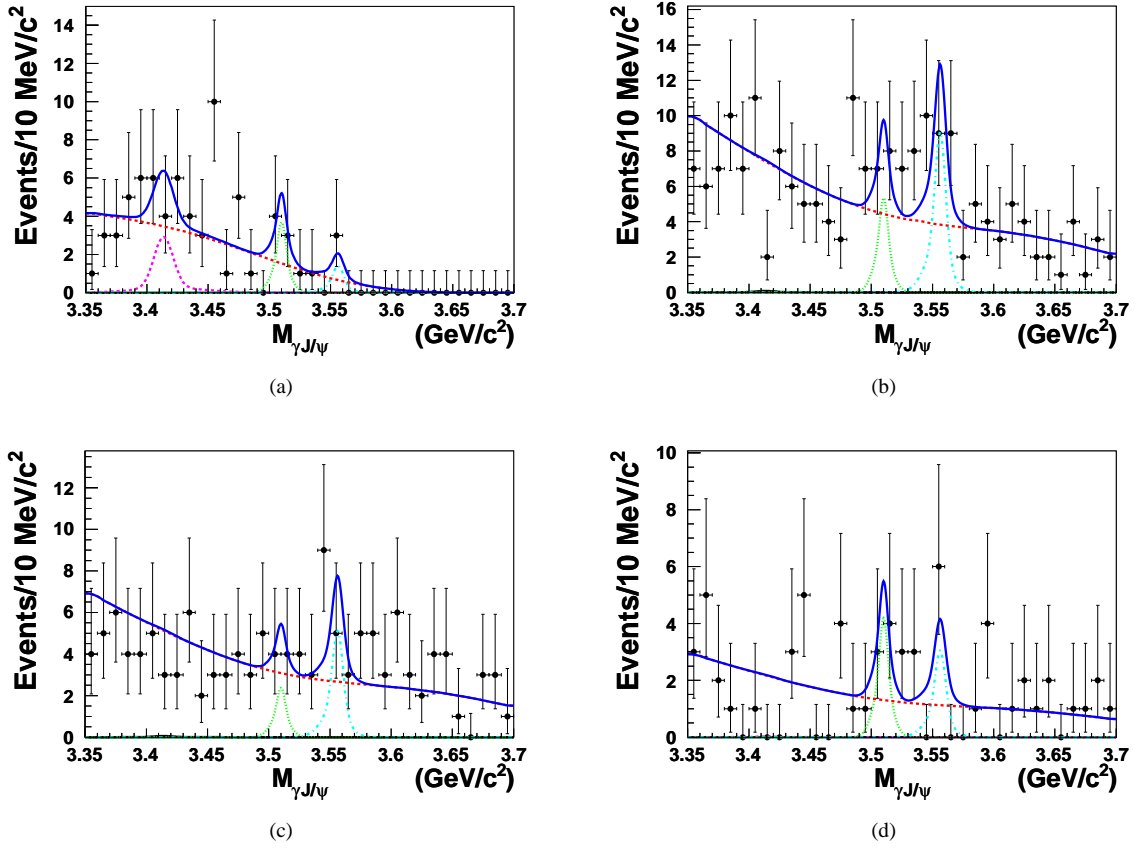


FIG. 2. The distribution of  $\gamma J/\psi$  invariant mass,  $M_{\gamma J/\psi}$ , and fit results for data at  $\sqrt{s} = 4.009$  (a), 4.230 (b), 4.260 (c) and 4.360 GeV (d). The solid lines show the total fit results. The  $\chi_{cJ}$  signals are shown as dashed lines, dotted lines, and dash-dotted lines, respectively, and the backgrounds are indicated by red dashed lines.

## VII. SYSTEMATIC UNCERTAINTIES

The systematic uncertainties in the cross section measurements of  $e^+e^- \rightarrow \gamma\chi_{cJ}$  caused by various sources are par-

tially in common for all channels. The common sources of systematics include the luminosity measurement, reconstruction efficiencies for charged tracks and photons, the vacuum polarization factor, kinematic fit and branching fractions of

TABLE II. The results on  $e^+e^- \rightarrow \gamma\chi_{cJ}$  Born cross section measurement. Shown in the table are the significance  $\sigma$ , detection efficiency  $\epsilon$ , number of signal events from the fits  $N^{\text{obs}}$ , radiative correction factor  $(1 + \delta^r)$ , vacuum polarization factor  $(1 + \delta^v)$ , upper limit (at the 90% C.L.) on the number of signal events  $N^{\text{UP}}$ , Born cross section  $\sigma^B$  and upper limit (at the 90% C.L.) on the Born cross section  $\sigma^{\text{UP}}$  at different CME point. The first uncertainty of the Born cross section is statistical, and the second systematic.

$\sqrt{s}$ (GeV)		$N^{\text{obs}}$	significance ( $\sigma$ )	$N^{\text{UP}}$	$\epsilon$ (%)	$1 + \delta^r$	$1 + \delta^v$	$\sigma^{\text{UP}}$ (pb)	$\sigma^B$ (pb)
4.009	$\chi_{c0}$	$7.0 \pm 6.6$	1.6	18	$36.4 \pm 0.2$	0.738	1.04	182	$65.0 \pm 61.3 \pm 5.3$
	$\chi_{c1}$	$4.4 \pm 2.6$	2.2	9	$23.4 \pm 0.1$			5.3	$2.4 \pm 1.4 \pm 0.2$
	$\chi_{c2}$	$1.8 \pm 1.7$	1.5	6	$8.7 \pm 0.1$			18	$4.7 \pm 4.4 \pm 0.6$
4.230	$\chi_{c0}$	$0.2 \pm 2.3$	0.0	7	$37.2 \pm 0.2$	0.840	1.06	26	$0.7 \pm 8.0 \pm 0.1$
	$\chi_{c1}$	$6.7 \pm 4.3$	1.9	14	$44.4 \pm 0.2$			1.7	$0.7 \pm 0.5 \pm 0.1$
	$\chi_{c2}$	$13.3 \pm 5.2$	2.9	22	$42.0 \pm 0.2$			5.0	$2.7 \pm 1.1 \pm 0.3$
4.260	$\chi_{c0}$	$0.1 \pm 1.9$	0.0	5	$36.7 \pm 0.2$	0.842	1.06	26	$0.5 \pm 8.8 \pm 0.1$
	$\chi_{c1}$	$3.0 \pm 3.0$	1.1	7	$42.7 \pm 0.2$			1.1	$0.4 \pm 0.4 \pm 0.1$
	$\chi_{c2}$	$7.5 \pm 3.9$	2.3	14	$41.7 \pm 0.2$			4.2	$2.0 \pm 1.1 \pm 0.2$
4.360	$\chi_{c0}$	$0.1 \pm 0.7$	0.0	3	$32.4 \pm 0.2$	0.943	1.05	23	$0.7 \pm 5.0 \pm 0.1$
	$\chi_{c1}$	$5.2 \pm 4.9$	2.4	10	$31.7 \pm 0.2$			2.9	$1.4 \pm 1.3 \pm 0.1$
	$\chi_{c2}$	$4.4 \pm 4.5$	2.0	9	$30.3 \pm 0.2$			5.0	$2.3 \pm 2.3 \pm 0.2$

TABLE III. Summary of systematic uncertainties at  $\sqrt{s} = 4.009, 4.230, 4.260$ , and  $4.360$  GeV(%).

$\sqrt{s}$ (GeV)	4.009			4.230			4.260			4.360		
Sources	$\chi_{c0}$	$\chi_{c1}$	$\chi_{c2}$	$\chi_{c0}$	$\chi_{c1}$	$\chi_{c2}$	$\chi_{c0}$	$\chi_{c1}$	$\chi_{c2}$	$\chi_{c0}$	$\chi_{c1}$	$\chi_{c2}$
Luminosity	1.0	1.0	1.0	1.0	1.0	1.0	1.0	1.0	1.0	1.0	1.0	1.0
Tracking efficiency	2.0	2.0	2.0	2.0	2.0	2.0	2.0	2.0	2.0	2.0	2.0	2.0
Photon detection	2.0	2.0	2.0	2.0	2.0	2.0	2.0	2.0	2.0	2.0	2.0	2.0
Kinematic fit	0.6	0.6	0.6	0.6	0.6	0.6	0.6	0.6	0.6	0.6	0.6	0.6
Branching ratio	4.8	3.6	3.7	4.8	3.6	3.7	4.8	3.6	3.7	4.8	3.6	3.7
Vacuum polarization factor	0.5	0.5	0.5	0.5	0.5	0.5	0.5	0.5	0.5	0.5	0.5	0.5
$\chi_{cJ}$ mass resolution	0.3	2.0	7.4	0.0	7.7	7.8	0.0	4.3	6.5	0.0	1.1	2.0
$\chi_{cJ}$ mass	0.0	0.9	1.4	0.0	0.3	0.2	0.0	0.1	0.1	0.0	0.3	0.4
Decay mode	4.9	2.2	3.9	5.5	1.2	3.3	5.9	1.9	2.9	5.1	1.5	2.1
Fit range	0.1	2.2	2.6	0.0	1.5	2.3	0.0	3.1	2.5	0.0	3.0	3.7
Background shape	0.0	3.1	5.6	0.0	0.7	0.3	0.0	1.1	0.4	0.0	0.9	0.1
Radiative correction factor	3.0	2.7	3.6	2.6	3.1	2.1	3.5	2.1	2.5	1.8	3.4	3.8
Total	8.1	7.3	12.1	8.3	9.8	10.2	8.9	7.7	9.3	7.9	6.9	7.7

the decay of the intermediate states. The systematic uncertainty due to the luminosity measurement is estimated to be 1.0% using Bhabha events. The uncertainty related to the track reconstruction efficiency of high-momentum muons is 1.0% per track [26]. The systematic uncertainty related to the photon detection is estimated to be 1.0% per photon [14]. The systematic uncertainty due to 5C-fit is 0.6%, obtained by studying a control sample of  $\psi' \rightarrow \eta J/\psi$  decays. The uncertainty related to the branching fractions of  $\chi_{cJ}$  and  $J/\psi$  decays are taken from the PDG [21]. The uncertainty for the vacuum polarization factor is 0.5% [25].

The other systematic uncertainties arising from the  $\chi_{cJ}$

mass resolution, the shift of the  $\chi_{cJ}$  reconstructed mass, the MC model, the shape of background, the radiative correction factor and the fit range at different CME points are discussed below.

The  $\psi' \rightarrow \gamma\chi_{cJ}$  channel is employed as a control sample to extract the differences on the mass resolution of the  $\chi_{cJ}$  signal by fitting the  $M_{\gamma J/\psi}$  spectrum. The differences in the mass resolutions between data and MC are found to be 0.02%, 0.01%, 0.2% for  $\chi_{cJ}$  ( $J = 0, 1, 2$ ). A similar fit is performed, in which the signal shapes are smeared to compensate for the mass resolution difference, and the differences on the yields of  $\chi_{cJ}$  signal are taken as the systematic uncertainties due to

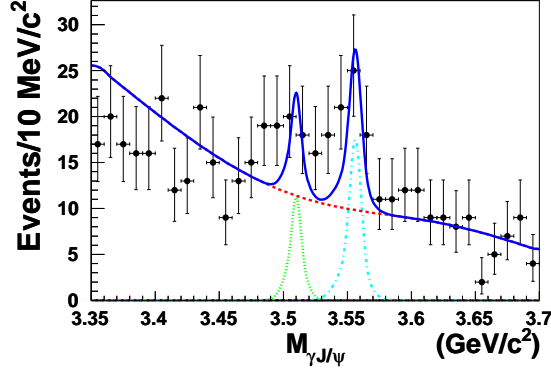


FIG. 3. Result of the simultaneous fit to  $M_{\gamma J/\psi}$  distributions for all CME data sets assuming that the signals are from decays of the  $Y(4260)$ . The blue solid line is the total fit result. The  $\chi_{cJ}$  signals are shown as dashed line, dotted line, and dash-dotted line, respectively, and the background is shown as the red dashed line.

the mass resolution.

An alternative fit is performed shifting the mean of  $\chi_{cJ}$  signal shapes by one standard deviation of the PDG values, and the deviations of the signal yields to the nominal values are taken as the systematic uncertainties due to the uncertainties of the signal line shapes.

The detection efficiency is evaluated using MC samples based on the E1 transition assumption [19] for  $Y(4260) \rightarrow \gamma\chi_{cJ}$ . Another set of MC samples is generated where the  $Y(4260) \rightarrow \gamma\chi_{cJ}$  decay is modeled using a phase space distribution, and the differences of the detector efficiencies between the two sets of MC samples are treated as systematic uncertainties from the MC model.

To estimate the systematic uncertainty related to the background shape, a control sample is selected from the data by requiring a  $\mu^+\mu^-$  pair and at least one photon. An alternative background shape is then extracted by re-weighting the  $\gamma\mu^+\mu^-$  invariant mass spectrum of the control sample, where the weights are the efficiency ratio of  $e^+e^- \rightarrow (n\gamma)\mu^+\mu^-$  MC simulated events surviving the signal selection criteria to the same selection criteria for the control sample. A fit with the alternative background shape is performed, and the differences between the yields of  $\chi_{cJ}$  signal to the nominal ones are taken as the systematic uncertainties due to the shape of background.

The possible distortions of the  $Y(4260)$  line shape due to interference effects with nearby resonances could introduce uncertainties in the radiative correction factor  $\epsilon \times (1 + \delta^r)$ . To estimate the related systematic uncertainties, we instead assume that  $e^+e^- \rightarrow \gamma\chi_{cJ}$  are produced via  $\psi(4040)$  decays at  $\sqrt{s} = 4.009$  GeV,  $\psi(4160)$  decays at  $\sqrt{s} = 4.229$  and 4.260 GeV, and  $\psi(4415)$  decays at  $\sqrt{s} = 4.360$  GeV. The variations in the factor  $\epsilon \times (1 + \delta^r)$  are taken as the systematic uncer-

tainties due to the radiative correction factor.

A series of similar fits are performed in different ranges of the  $M_{\gamma J/\psi}$  distribution, and the largest differences on the signal yields to the nominal values are taken as systematic uncertainties.

All the systematic uncertainties from the different sources are summarized in Table III. The total systematic uncertainties are calculated as the quadratic sum of all individual terms.

## VIII. SUMMARY

Using data samples collected at CME of  $\sqrt{s} = 4.009, 4.230, 4.260$ , and 4.360 GeV with the BESIII detector, we perform a search for  $e^+e^- \rightarrow \gamma\chi_{cJ}$  ( $J = 0, 1, 2$ ) with the subsequent decay  $\chi_{cJ} \rightarrow \gamma J/\psi$  and  $J/\psi \rightarrow \mu^+\mu^-$ . We find evidence for the processes  $e^+e^- \rightarrow \gamma\chi_{c1}$  and  $e^+e^- \rightarrow \gamma\chi_{c2}$  with statistical significances of  $3.0\sigma$  and  $3.4\sigma$ , respectively. No evidence of  $e^+e^- \rightarrow \gamma\chi_{c0}$  is observed. The corresponding Born cross sections of  $e^+e^- \rightarrow \gamma\chi_{cJ}$  at different CME are calculated and listed in Table II. Under the assumption of the absence of  $\chi_{cJ}$  signals, the upper limits on the Born cross sections at the 90% C.L. are calculated and listed in Table II, too. These upper limits on the Born cross section of  $e^+e^- \rightarrow \gamma\chi_{cJ}$  are compatible with the theoretical prediction from an NRQCD calculation [16].

## IX. ACKNOWLEDGEMENT

The BESIII collaboration thanks the staff of BEPCII and the IHEP computing center for their strong support. This work is supported in part by National Key Basic Research Program of China under Contract No. 2015CB856700; Joint Funds of the National Natural Science Foundation of China under Contracts Nos. 11079008, 11179007, U1232201, U1332201; National Natural Science Foundation of China (NSFC) under Contracts Nos. 10935007, 11121092, 11125525, 11235011, 11322544, 11335008; the Chinese Academy of Sciences (CAS) Large-Scale Scientific Facility Program; CAS under Contracts Nos. KJCX2-YW-N29, KJCX2-YW-N45; 100 Talents Program of CAS; INPAC and Shanghai Key Laboratory for Particle Physics and Cosmology; German Research Foundation DFG under Contract No. Collaborative Research Center CRC-1044; Istituto Nazionale di Fisica Nucleare, Italy; Ministry of Development of Turkey under Contract No. DPT2006K-120470; Russian Foundation for Basic Research under Contract No. 14-07-91152; U. S. Department of Energy under Contracts Nos. DE-FG02-04ER41291, DE-FG02-05ER41374, DE-FG02-94ER40823, DESC0010118; U.S. National Science Foundation; University of Groningen (RuG) and the Helmholtzzentrum fuer Schwerionenforschung GmbH (GSI), Darmstadt; WCU Program of National Research Foundation of Korea under Contract No. R32-2008-000-10155-0.

- 
- [1] B. Aubert *et al.* (BABAR Collaboration), Phys. Rev. Lett. **95**, 142001 (2005).
  - [2] Q. He *et al.* (CLEO Collaboration), Phys. Rev. D **74**, 091104(R) (2006).
  - [3] C. Z. Yuan *et al.* (Belle Collaboration), Phys. Rev. Lett. **99**, 182004 (2007).
  - [4] J. P. Lees *et al.* (BABAR Collaboration), Phys. Rev. D **86**, 051102 (2012).
  - [5] Z. Q. Liu *et al.* (Belle Collaboration), Phys. Rev. Lett. **110**, 252002 (2013).
  - [6] E. Eichten, K. Gottfried, T. Kinoshita, K. Lane, and T. Yan, Phys. Rev. D **17**, 3090 (1978); **21**, 203 (1980); T. Barnes, S. Godfrey, and E. S. Swanson, Phys. Rev. D **72**, 054026 (2005).
  - [7] L. Liu *et al.* (Hadron Spectrum Collaboration), JHEP, **1207**, 126 (2012).
  - [8] D. Ebert, R. N. Faustov, and V. O. Galkin, Phys. Lett. B **634**, 214 (2006).
  - [9] L. Maiani, V. Riquer, F. Piccinini, and A. D. Polosa, Phys. Rev. D **72**, 031502(R) (2005).
  - [10] X. Liu, X.-Q. Zeng, and X.-Q. Li, Phys. Rev. D **72**, 054023(R) (2005).
  - [11] C. Z. Yuan, P. Wang, and X. H. Mo, Phys. Lett. B **634**, 399 (2006).
  - [12] X. L. Wang *et al.* (Belle Collaboration), Phys. Rev. D **87**, 051101(R) (2013).
  - [13] T. E. Coan *et al.*, (CLEO Collaboration), Phys. Rev. Lett. **96**, 162003 (2006).
  - [14] M. Ablikim *et al.*, (BESIII Collaboration), Phys. Rev. Lett. **112**, 092001 (2014).
  - [15] L. Ma, Z. F. Sun, X. H. Liu, W. Z. Deng, X. Liu and S. L. Zhu, Phys. Rev. D **90**, 034020 (2014).
  - [16] K. -T. Chao, Z. -G. He, D. Li and C. Meng, arXiv:1310.8597 [hep-ph].
  - [17] M. Ablikim *et al.* (BESIII Collaboration), Nucl. Instrum. Meth. A **614**, 345 (2010).
  - [18] S. Agostinelli *et al.* (GEANT4 Collaboration), Nucl. Instrum. Meth. A **506**, 250 (2003).
  - [19] D. J. Lange, Nucl. Instrum. Meth. A **462**, 152 (2001); R. G. Ping, HEP and NP **32**, 599602 (2008).
  - [20] S. Jadach, B. F. L. Ward and Z. Was 2000 Comp. Phys. Commu. **130**, 260; S. Jadach, B. F. L. Ward and Z. Was, Phys. Rev. D **63**, 113009 (2001).
  - [21] J. Beringer *et al.*, (Particle Data Group), Phys. Rev. D **86**, 010001 (2012).
  - [22] R. G. Ping, Chinese Phys. C **32**, 599 (2008).
  - [23] T. Sjostrand, L. Lonnblad and S. Mrenna, hep-ph/0108264.
  - [24] E. A. Kuraev and V. S. Fadin, Sov. J. Nucl. Phys. **41**, 466 (1985) [Yad. Fiz. **41**, 733 (1985)].
  - [25] S. Actis *et al.*, Eur. Phys. J. C **66**, 585 (2010).
  - [26] M. Ablikim *et al.* (BESIII Collaboration), Phys. Rev. D **86**, 071101 (2012).